

# Multi-Parameter Segmentation of Brain Images

Atam P. Dhawan and Brian D'Alessandro  
Department of Electrical and Computer Engineering  
New Jersey Institute of Technology  
Newark, NJ 07102, USA

**Abstract**— Recent advances in multi-parameter MR brain imaging has enabled multi-class tissue characterization for better quantitative analysis and understanding brain disorders and pathologies. This paper presents a maximum likelihood based method for multi-class segmentation that utilizes spatio-frequency features obtained from wavelet analysis along with the multi-parameter measurements. Results on MR brain images of a patient with stroke are presented.

**Keywords**- Multi-parameter segmentation, brain image analysis, tissue characterization.

## I. INTRODUCTION

Multi-class segmentation among conventional MRI, fMRI and DTI brain images for specific volumes of interests provides tissue characterization with associated pathologies for important quantitative analysis for diagnosis as well therapeutic intervention. Fusion of anatomical, functional and diffusion information usually leads to multi-dimensional data sets leading to analysis of local regions that can be obtained from segmentation and detection approaches based on multi-class classification.

Multi-modality multi-parameter brain imaging has been of significant interest to acquire detailed information about the anatomical features and functional behavior of brain tissues. With advances in brain MR imaging, new methods for volumetric image registration, mapping and segmentation analysis have been largely investigated [1-4]. Along with imaging, multi-class tissue characterization methods for adaptive learning of associated pathologies has been a continued objective for applications in diagnosis and therapeutic protocols related to critical brain disorders and diseases [5-6].

In this paper, an adaptive learning based multi-class segmentation method is presented that utilizes voxel-based measurements and spatio-frequency features obtained from wavelet analysis. Results with multi-parameter MR brain images of a stroke patient are presented and shown that new classes with characteristic pathologies can be learned and classified for follow-up analysis.

## II. MULTI-CLASS CLASSIFICATION USING MAXIMUM LIKELIHOOD DISCRIMINANT FUNCTIONS

Multi-parameter imaging and segmentation analysis leads to feature analysis with a set of spatially distributed multi-

dimensional data vectors of raw measurements and computed features. Total number of measurements and computed features allocated to each pixel in the image sets up the dimension  $d$  of the feature space. Let us assume that we have an image of  $m$  rows and  $n$  columns with  $mn$  number of pixels to be classified into  $k$  number of classes. Thus we have  $mn$  data vectors  $\mathbf{X} = \{\mathbf{x}_j; j = 1, 2, \dots, mn\}$  distributed in a  $d$ -dimensional feature space. Thus each element of the data vector (i.e., pixel in the image) is associated with  $d$ -dimensional feature vector. The purpose of multi-class classification is to find a mapping  $f(\mathbf{X})$  to map the input data vectors into  $k$  classes denoted by  $C = \{c_i; i = 1, 2, \dots, k\}$ . In order, to learn such a mapping, we can use a training set  $S$  of cardinality  $l$  with labeled input vectors such that

$$S = \{(\mathbf{x}_1, c_1), \dots, (\mathbf{x}_l, c_l)\} \quad (1)$$

$\mathbf{x}_i \in \mathcal{X}$  are provided in the inner-product space of  $\mathcal{X} \subseteq \mathbf{R}^d$  and  $C_i \in \mathcal{Y} = \{1, \dots, k\}$  the corresponding class or category label.

As shown in Equation (1), there is a pair relationship of the assignment of each input pixel  $X$  to a class  $C$ . Let us assume that each class  $c_i$  model obtained from the training set has a mean vector  $\mu_i$  and a co-variance represented by  $\hat{\Sigma}_i$  such that

$$\hat{\mu}_i = \frac{1}{n} \sum_j \mathbf{x}_j \quad (2)$$

where  $i=1, 2, \dots, k$ ; and  $j=1, \dots, n$ ;  $n$  is the number of pixel vectors in the  $i^{\text{th}}$  class, and  $\mathbf{x}_j$  is the  $j^{\text{th}}$  of  $n$  multidimensional vectors that comprise the class. The dimension of  $x_j$  corresponds to the number of image modalities used in the analysis. The covariance matrix of class  $i$ ,  $\hat{\Sigma}_i$ , is

$$\hat{\Sigma}_i = \frac{1}{n-1} \sum_j (\mathbf{x}_j - \hat{\mu}_i)(\mathbf{x}_j - \hat{\mu}_i)^t \quad (3)$$

For developing an estimation model [1-3], let us assume that the image to classify is a realization of a pair of random variables  $\{C_{mn}, X_{mn}\}$ ; where  $C_{mn}$  is the class of the pixel  $mn$ .  $C_{mn}$  represents the spatial variability of the class in the image and can take the values in a discrete set  $\{1, 2, \dots, k\}$ .  $X_{mn}$  is a  $d$ -dimensional random variable of pixel  $mn$  describing the variability of measurements for that pixel.  $X_{mn}$  describes the variability of the observed values  $\mathbf{x}$  in a particular class. Given that  $C_{mn} = i$ , ( $i=1,2,\dots,k$ ) the distribution of  $X_{mn}$  is estimated to obey the general multivariate normal distribution described by the density function

$$\hat{p}_i(\mathbf{x}) = \frac{1}{(2\pi)^{d/2} |\hat{\Sigma}_i|^{1/2}} \exp\left[\frac{-(\mathbf{x} - \hat{\mu}_i)}{2\hat{\Sigma}_i(\mathbf{x} - \hat{\mu}_i)}\right] \quad (4)$$

where  $\mathbf{x}$  is a  $d$ -element column vector,  $\hat{\mu}_i$  is a  $d$ -element estimated mean vector for the class  $i$  calculated from the training set,  $\hat{\Sigma}_i$  is the estimated  $d \times d$  covariance matrix for class  $i$  also calculated from the training set, and  $d$  is the dimension of multi-parameter or feature vector.

For Maximum Likelihood based discriminant analysis to assign a class to a given pixel in the image [1-4]. For each pixel, four transition matrices  $P_r(m,n) = [p_{ijr}(m,n)]$  can be estimated, where  $r$  is a direction index (following 4 spatial connectedness directions in the image) and  $p_{ijr}(m,n)$  are the transition probabilities defined by

$$p_{ij1}(m,n) = P\{C_{mn} = j | C_{m,n-1} = i\} \quad (5)$$

$$p_{ij2}(m,n) = P\{C_{mn} = j | C_{m+1,n} = i\} \quad (6)$$

$$p_{ij3}(m,n) = P\{C_{mn} = j | C_{m,n+1} = i\} \quad (7)$$

$$p_{ij4}(m,n) = P\{C_{mn} = j | C_{m-1,n} = i\}. \quad (8)$$

A generalized estimation of transition probabilities for classes can be obtained using  $b$  images in the training set and averaged over small neighborhood of  $h$  pixels around the pixel  $mn$  as

$$p_{ij1}(m,n) = \frac{\sum_b \sum_n \{\text{pix} | C_{mn} = j, C_{m,n-1} = i\}}{\sum_b \sum_n \{\text{pix} | C_{m,n-1} = i\}}$$

$$p_{ij2}(m,n) = \frac{\sum_b \sum_n \{\text{pix} | C_{mn} = j, C_{m+1,n} = i\}}{\sum_b \sum_n \{\text{pix} | C_{m+1,n} = i\}}$$

$$p_{ij3}(m,n) = \frac{\sum_b \sum_n \{\text{pix} | C_{mn} = j, C_{m,n+1} = i\}}{\sum_b \sum_n \{\text{pix} | C_{m,n+1} = i\}}$$

$$p_{ij4}(m,n) = \frac{\sum_b \sum_n \{\text{pix} | C_{mn} = j, C_{m-1,n} = i\}}{\sum_b \sum_n \{\text{pix} | C_{m-1,n} = i\}} \quad (9)$$

where  $\Sigma_b\{\text{pix} | CP\}$  denotes the number of pixels with the property  $CP$  in the images used in the training set used to generate the model and  $\Sigma_n$  represents the number of pixels with the given property in the pre-defined neighborhood.

The equilibrium transition probabilities can then be estimated using a similar procedure as

$$\pi_i(mn) = \frac{\sum_b \sum_n \{\text{pix} | C_{mn} = i\}}{\sum_b \sum_n \{\text{pix}\}}. \quad (10)$$

The probability of a pixel,  $mn$  belonging to class  $i$  given the characteristics of the pixels in the neighborhood of  $mn$  can now be defined as

$$P\{C_{mn} = i | \mathbf{x}_{kl}, (k,l) \in N(m,n)\} = \frac{P\{C_{mn} = i | X_{mn}\} P\{X_{mn}\} H_{m-1,n}(i) H_{m,n-1}(i) H_{m+1,n}(i) H_{m,n+1}(i)}{P\{X_{mn} | X_{m\pm 1,n}, X_{m,n\pm 1}\} P\{X_{m\pm 1,n}, X_{m,n\pm 1}\}} \quad (11)$$

Pixels are classified based on the class that maximizes. It is important to develop an efficient data vector for use in classification method. Within the neighborhood of pixel  $mn$ , both direct measurements from multi-parameter imaging protocol as well as computed spatio-frequency features as obtained from wavelet analysis

### III. MODEL AND FEATURE EXTRACTION

The model developed in [6] employed 15 brain tissue classes instead of the commonly used set of four classes, which were of clinical interest to neuroradiologists for following-up with patients suffering from cerebrovascular deficiency (CVD) and/or stroke. The model approximates the spatial distribution of tissue classes by a Gaussian Markov random field and uses maximum likelihood method to estimate the class probabilities and transitional probabilities for each pixel of the image. Multi-parameter MR brain images with  $T_1$ ,  $T_2$ , proton density,  $Gd+T_1$ , and perfusion imaging were used in segmentation and classification. In the development of the segmentation model, true class-membership of measured parameters was determined from manual segmentation of a set of normal and pathologic brain images by a team of neuroradiologists.

An initial set of 15 tissue classes, as shown in Table 1 was identified by the neuroradiologist. Gray matter was divided into superficial and deep gray mater structures because pathologic processes often discriminate between involvement of the superficial cortical or deep basal ganglia. The deep gray matter was further divided into four classes, caudate head, putamen, globus pallidus, and thalamus. White matter was divided into three classes: superficial white matter and two deeper white matter tracts, the corpus callosum and the internal capsule. The superficial white matter consisted primarily of white matter within the cortical pathways of the centrum semiovale. The CSF spaces were divided into two classes based on the ventricular system. The first class was that of the CSF contained within the ventricular system and the second class was for CSF outside the ventricular system (within the extra-axial spaces). This selection is based on the understanding that CSF within the ventricular system may have some signal variation due to the influence of pulsatile blood flow.

CLASS NUMBER	Color Code	Class Name
C1	White	White Matter
C2	Yellow	Corpus Callosum
C3	Gray	Superficial Gray
C4	Blue Green	Caudate
C5	Blue	Thalamus
C6	Light Blue	Putamen
C7	Dark Blue	Globus Pallidus
C8	Light Cream	Internal Capsule
C9	Light Violet	Blood Vessel
C10	Dark Violet	Ventricle
C11	Dark Green	Choroid Plexus
C12	Green	Septum Pellucidum
C13	Pale Green	Fornices
C14	Orange	Extraaxial Fluid
C15	Pale Violet	Zona Granularis

Table 1. List of classes used in proposed classification scheme.

New Classes #	Name
C16	Superficial gray-edema (red gray)
C17	Infarction (red)
C18	Abnormal white matter (rose)
C19	Internal capsule/edema (cream rose)
C20	Putamn edema (blue rose)
C21	Globus pallidus/edema (blue violet)

Table 2: New 6 Pathological classes learned through the MAS method.

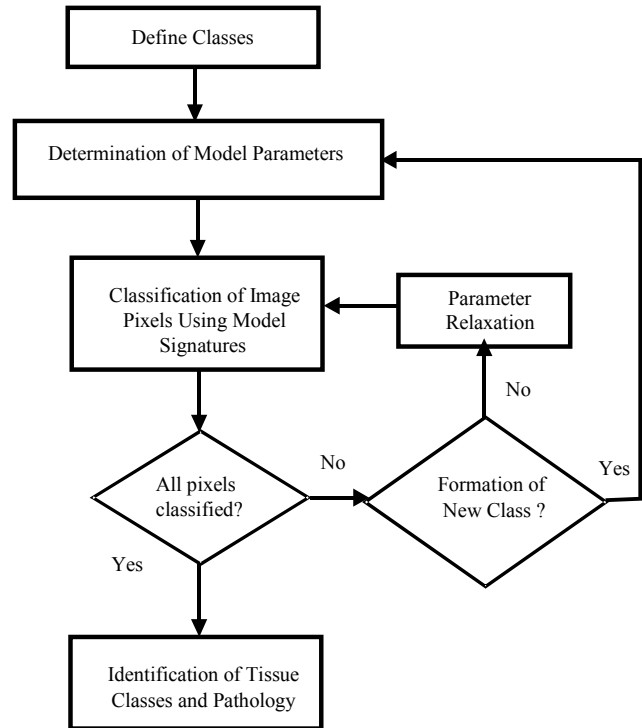


Figure 1. A schematic flow chart of the multi-parameter segmentation method [ref. 5]

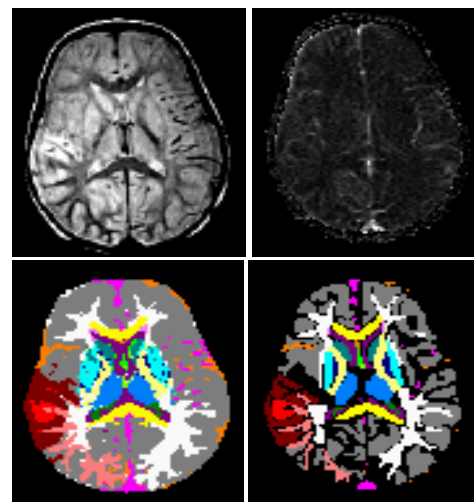


Figure 2. From Top left clockwise: Proton Density MR slice brain image of a patient with 48 hours after the stroke, Perfusion MR image, manual segmentation by neuroradiologists, and results of automatic segmentation method.

The feature vector from raw images (T1, T2, PD, Gd, Perfusion) was then augmented with coefficients obtained from the wavelet decomposition. Three-level wavelet decomposition was used using Daubechies dB8 wavelet [7-8].

Using the Maximum Likelihood discriminant function method described above, MR brain images were analyzed and segmented into 15 classes using multi-class classification approach. Five complete sets of MR T1-weighted, T-2 weighted, Proton Density, Gd+T1-weighted and Perfusion brain images were used to determine the class signatures. These images were obtained at 1 mm interslice and 5 mm intra-slice resolution. The images with no observed pathology were used in manual classification by two expert neuroradiologists for a 15-class classification. After the signatures were created using the complete feature vector including raw data and computed wavelet coefficients, a new data set of respective images from a patient with stroke was analyzed using the signature database. Figure 1 shows a flowchart of the classification process.

#### IV. RESULTS AND DISCUSSION

Figure 2 shows PD and Perfusion MR brain images of the patient with stroke in the top row. The bottom row shows results of automatic classification with 4x4 pixel probability cell size and 4 pixel wide averaging along with a manual segmentation that was obtained using two neuroradiologists for comparison. Table 2 shows new classes that were created using the above described method along with its pathological classification.

It can be seen that new classes relevant to the pathology were learned by the presented method. The contribution and significance of spatio-frequency information obtained from the wavelet decomposition needs to be further investigated for its robustness in classification of pathology.

#### ACKNOWLEDGEMENT

Authors are grateful to neuro-radiologists Drs. Mary Gaskill-Shiple and William Ball for providing data, manual segmentation and pathology interpretation. Some of the work on maximum likelihood discriminant analysis was done by Aleksandar Zavaljevski for his Ph.D. dissertation.

#### REFERENCES

- [1] Davatzikos, C., A. Genc, D. Xu, and S.M. Resnick, "Voxel-Based Morphometry Using the RAVENS Maps: Methods and Validation Using Simulated Longitudinal Atrophy". *NeuroImage*, 2001, **14**(6): p. 1361-1369.
- [2] Z. Xue, D. Shen and C. Davatzikos "Determining correspondence in 3-D MR brain images using attribute vectors as morphological signatures of voxels," *IEEE Trans. Med. Imag.*, vol. 23, pp. 1276, Oct. 2004.
- [3] P. Yushkevich, J. Piven, H. Hazlett, R. Smith, S. Ho, J. Gee and G. Gerig "User-guided 3-D active contour segmentation of anatomical structures: Significantly improved efficiency and reliability," *NeuroImage*, vol. 31, pp. 1116, 2006.
- [4] W. L. Nowinski, G. Y. Qian, K. N. Bhanu Prakash, A. Thirunavukarasu, Q. Hu, N. Ivanov, A. S. Parimal, V. L. Runge and N. J. Beauchamp "Analysis of ischemic stroke MR images by means of brain atlases of anatomy and blood supply territories," *Acad. Radiol.*, vol. 13, pp. 1025, 2006.
- [5] Zavaljevski, A., A.P. Dhawan, S. Holland, W. Ball, M. Giskill-Shiple, J. Johnson and S. Dunn, "Multispectral MR brain image classification", *Computerized Medical Imaging, Graphics and Image Processing*, 24, pp. 87-98, 2000.
- [6] Clarke, L., R. Velthuizen, S. Phuphanich, J. Schellenberg, J. Arrington, and M. Silbiger, MRI: stability of three supervised segmentation techniques. *Magnetic Resonance Imaging*, 11: p. 95-106, 1993.
- [7] Ingrid Daubechies, *Ten Lectures on Wavelets*, Society for Applied Mathematics, Philadelphia, PA, 1992.
- [8] S. Patwardhan, S. Dai, and A.P. Dhawan, "Multispectral Image Analysis and Classification of Melanoma using Fuzzy Membership based Partitions" *Computerized Medical Imaging and Graphics*, vol. 29, pp. 287-296, 2005.